On-line coupling of flow field-flow fractionation and multi-angle laser light scattering

Dierk Roessner, Werner-Michael Kulicke*

Institut für Technische und Makromolekulare Chemie, Universität Hamburg, Bundesstrasse 45, 20146 Hamburg, Germany

Abstract

This paper describes the first successful coupling of a flow field-flow fractionator with a multi-angle laser light-scattering photometer in order to carry out absolute measurements of even high molar mass and radius of gyration distributions. Two standards with broad molar mass distributions, polystyrene particles and coil-shaped dissolved dextrans were investigated in order to establish the efficiency of this experimental apparatus. The distribution functions of molar mass and radius of gyration were determined for the samples. The results calculated for the dextran sample from the distribution functions were a weight-average molar mass of 2 730 000 g/mol and a z-average radius of gyration of 47 nm. Comparison with results obtained from a conventional apparatus, consisting of size-exclusion chromatography and a light-scattering photometer, showed that field-flow fractionation is able to separate molecules in the range where size-exclusion chromatography fails owing to the existence of an exclusion boundary. The polystyrene latex sample gave results of 13 400 000 g/mol for the weight-average molar mass and 15 nm for the z-average radius of gyration. In addition, a structure–property relationship in the form of an $\langle R_G^2 \rangle^{1/2}$ versus M relationship was calculated for each substance. For the polystyrene latex standard in water an exponent of 0.33 ± 0.02 was found. The corresponding value for the dextran in $0.1\ M$ sodium nitrate solution was 0.50 ± 0.01.

1. Introduction

In view of the increasing interest in water-soluble polymers, which results from their numerous applications, there is a great demand for information on the steric structure of these substances, which holds for both non-ionic [1,2] and ionic [1,3–5] polymers. The steric structure may be described by distributions or average values of the molar masses and radii. One example of an application where a knowledge of these parameters is important is the clinical use of polymeric substances as plasma expanders for restoring the volume and improving the flow behaviour of blood. Solutions of hydroxyethyl starch or dextran in electrolytic solutions isotonic with the blood are used for this purpose. These polymers, the structures of which affect the pharmacokinetics and pharmacology of the preparation, can be fractionated by means of size-exclusion chromatography (SEC) and thus be characterized in more detail [6,7].

However, this established method of fractionation is subject to certain restrictions that prevent the characterization of polymer molecules strongly adsorbed by the packing material in the column. In addition, large polymer molecules can be excluded from fractionation or degraded

---

* Corresponding author.

even at low flow-rates [8]. These problems occur for a large number of high-molar-mass, water-soluble polymers with interesting technical applications. Examples of these are the synthetic high-molar-mass polyelectrolytes used in industrial chemistry as flocculating agents for clarifying sludges [9], or cellulose derivatives [10] used in building materials, foodstuffs, paper, cosmetics and pharmaceuticals. Such polymers can exceed a radius of gyration of more than 200 nm [3] and consequently they are excluded because of their hydrodynamic volume, and therefore cannot be fractionated by size-exclusion chromatography.

Field-flow fractionation (FFF) was developed in order to fractionate substances for which size-exclusion chromatography is not effective. As demonstrated by Giddings and co-workers, it is a method for rapidly and efficiently fractionating high-molar-mass macromolecules and particles. Three different methods of field-flow fractionation have proved to be successful: sedimentation field-flow fractionation [11–13], thermal field-flow fractionation [14–16] and flow field-flow fractionation [17–19] (FFFF). The advantages of these fractionation techniques lie in their lack of sensitivity to adsorption [20] and in their extremely high upper working limit of particle diameters of ca. 50 μm [21].

The aim of our investigations was to establish whether the FFFF method could be coupled with a multi-angle laser light-scattering photometer for absolute measurement of masses and radii, thus obviating the need for any calibration with polymer standards or a universal elution curve. Successful coupling of FFFF with multi-angle laser light scattering (MALLS) would have the advantage of permitting the analytical fractionation of even problematic, high-molar-mass polymers and the on-line determination of molar masses and radii of gyration. In addition, the concentration of each of the species to be eluted can be measured by means of a differential refractometer. In this way, from a single experiment, it should be possible to carry out determinations of the distributions of molar mass and radius of gyration together with their mean values and to establish a structure-property relationship [22].

2. Theory

2.1. Multi-angle laser light scattering

Light scattering is one of a few methods available for the absolute determination of molar mass and structure and is certainly applicable over the broadest range of molar mass of any method. Early developments of the theory of light scattering from macromolecular solutions and suspensions were made by Einstein [23], Raman [24], Debye [25] and Zimm [26].

Values for the molar mass M and radius of gyration $\langle R_G^2 \rangle^{1/2}$ at each slice across the distribution were calculated using the usual light scattering equations:

$$\frac{Kc}{R_\vartheta} = \frac{1}{M_W P_{(\vartheta)}} + 2A_2 c \qquad (1)$$

where

$$K = \frac{4\pi^2 n_0^2}{N_A \lambda_0^4} \left(\frac{dn}{dc}\right)^2 \qquad (2)$$

$$R_\vartheta = \frac{r^2 I_\vartheta}{I_0 V} \qquad (3)$$

$$P_{(\vartheta)}^{-1} = 1 + \frac{\langle R_G^2 \rangle_z q^2}{3} \qquad (4)$$

$$q = \frac{4\pi n_0}{\lambda_0} \cdot \sin\left(\frac{\vartheta}{2}\right) \qquad (5)$$

This equation incorporates the light-scattering constant for vertically polarized incident light, K, which contains the refractive index increment dn/dc, the concentration, c, the Rayleigh ratio, R_ϑ, at the scattering angle ϑ, the weight-average molar mass, M_w, and the second virial coefficient A_2. The Rayleigh ratio, R_ϑ, is used to obtain a parameter for the scattered light intensity that is independent of the measuring conditions. The function $P_{(\vartheta)}$ describes the angular dependence of the scattered light intensity. For small angles it is only dependent on the radius of gyration and not on factors such as molecular conformation or branching.

Irrespective of the fractionation method, one must assume that in a fractionation experiment on polymers with a unique relationship between molar mass and radius of gyration and elution

volume, the distribution within a given element of the elution volume is so negligibly small that the weight-average molar mass and the z-average radius of gyration become equivalent to the values for a monodisperse sample.

2.2. Flow field-flow fractionation

The essential component of a field-flow fractionator is the so-called channel. In the case of FFFF, it consists of two Perspex blocks fitted with ceramic frits and a semi-permeable membrane. Between these blocks there is a spacer with the cut-out channel. Two currents are generated in the channel: the channel flow, $\dot{V}$, along the block and the cross flow, $\dot{V}_x$, perpendicular to the channel flow using the frits installed in the channel. The perpendicular or external field forces the various species of the sample into different flow layers of the laminar channel flow, where they are transported at different velocities and thus only separated according to their diffusion coefficients.

The mathematical formulation of the elution behaviour of polymers and particles during field-flow fractionation and especially during flow field-flow fractionation has been discussed in detail in a number of publications [27–29]. For flow field-flow fractionation in the normal mode the following equation applies to the retention time of a species, t_R:

$$t_R = \frac{w^2}{6D} \cdot \frac{\dot{V}_x}{\dot{V}} \qquad (6)$$

From Eq. 6 it can be seen that the retention time, t_R, of a species is directly proportional to the square of the channel thickness, w, and inversely proportional to the diffusion coefficient, D, of the species. There is also a direct proportionality with the quotient of cross flow, $\dot{V}_x$, and channel flow, $\dot{V}$. This indicates that the retention time of a species can be varied by altering the channel flow or cross flow. The diffusion coefficient can be used for calculating the molecular dimensions in the form of the Stokes diameter, d_S. The mathematical basis for this is provided by the Stokes–Einstein equation shown in Eq. 7.

$$D = \frac{kT}{3\pi\eta d_S} \qquad (7)$$

$$t_R = \frac{\pi\eta w^2}{2kT} \cdot \frac{\dot{V}_x}{\dot{V}} \cdot d_S \qquad (8)$$

Eq. 8, which can be formed by linking Eqs. 6 and 7, gives the dependence of the retention time, t_R, on the material and experimental parameters. FFF enables diffusion coefficients and particle dimensions to be measured absolutely. In the case of homogeneous, spherical particles, the molar mass can also be determined absolutely in this way. For coil-shaped polymers in solution, FFFF yields relatively determined molar masses [30]. For this reason, the absolute method of light scattering was employed to determine molar mass, thus obviating the need for calibration with polymer standards.

3. Experimental

The FFFF experiments were carried out with a Model F-1000 Universal Fractionator, manufactured by FFFractionation (Salt Lake City, UT, USA). A schematic representation of the experimental apparatus is given in Fig. 1. The dimensions of the channel were 28.5 cm long, 2.0
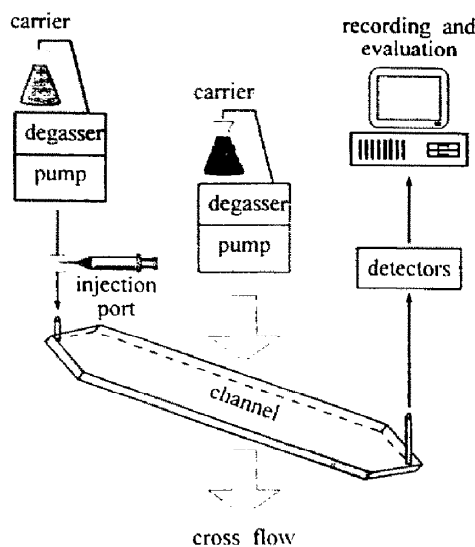

Fig. 1. Schematic representation of FFFF–MALLS apparatus.

cm wide and 0.025 cm thick. Two HPLC pumps
were employed to generate the current of the
carrier liquid. The volume flows were monitored
gravimetrically. The polystyrene sample was
specially provided for the experiments by
FFFractionation. FFFF experiments with this
sample used doubly distilled water containing
0.02% (w/w) sodium azide and 0.05% (w/w)
sodium dodecyl sulphate as the carrier liquid.
The FFFF experiments on the polysaccharide
dextran (Pfeifer and Langen Pharma) were car-
ried out in a 0.1 M sodium nitrate solution
containing 0.02% (w/w) of sodium azide.

Size-exclusion chromatography employed TSK
60/50/40/30 PW XL columns (Toyo Soda),
arranged in order of decreasing pore size. The
columns were conditioned in a column heater at
295 K. The flow-rate was 1 ml min^{-1}. The
solvent used was doubly distilled water contain-
ing 0.1 M sodium nitrate and 0.02% (w/w)
sodium azide. A 100-μl injection loop and a
$1 \cdot 10^{-3}$ g ml^{-1} solution of dextran were used.

Concentration detection was performed with a
Shodex RI SE-51 differential refractometer
manufactured by Showa Denko (Tokyo, Japan).
Detection of scattered light was carried out with
a Watt Technologies (Santa Barbara, CA, USA)
Dawn-F multi-angle laser light-scattering photo-
meter. The instrument was operated with verti-
cally polarized light of wavelength 632.8 nm at a
temperature of 295 K. The light-scattering
photometer was calibrated with toluene. The
normalization coefficients were measured with
gold dispersion. The spider-plot method with
narrowly distributed standards was used to mea-
sure the interdetector volume [31]. The signal
from the differential refractometer was routed to
the Dawn-F, which was interfaced to an AT
computer. Software from Wyatt Technologies
was used to analyse the data.

4. Results and discussion

4.1. Fractionation of a particle dispersion

Lattices are dispersions of spherical polymer
particles manufactured by emulsion polymeriza-

tion. They are characterized by a low viscosity,
even at high concentrations, and are used on a
large commercial scale for the manufacture of
paints, impregnating agents and adhesive pastes.

The results of the FFFF–MALLS experiments
on the polystyrene latex standard B1 are summa-
rized in Figs. 2–5 and Tables 1 and 2. In Fig. 2
the radii of gyration calculated from the initial
curves of the scattering functions are plotted as a
function of the elution volume.

The fluctuation of the data points at small
elution volumes is the result of the fact that the
particle dimensions in this area are approximate-
ly $<\lambda/20$. For such small particles the angular
dependence of $P(\vartheta)$ becomes unimportant since
the scattering is essentially isotropic, and one is
therefore unable to determine the radius of
gyration. According to the equation

$$d_{\text{LS}} = \sqrt{\frac{20}{3}} \cdot \langle R_{\text{G}}^2 \rangle^{1/2} \qquad (9)$$

which relates spherical particle dimensions to the
radius of gyration, the lowest radius that can be
measured is about 9 nm. In the range of higher
elution volumes there is a fluctuation of data
points because of the weak signals of the photo-
diodes.

By including the concentration, which was
measured on-line with the differential refrac-
tometer for each of the eluates investigated, it is
possible to calculate the radius of gyration dis-
tribution shown in Fig. 3. The range that could
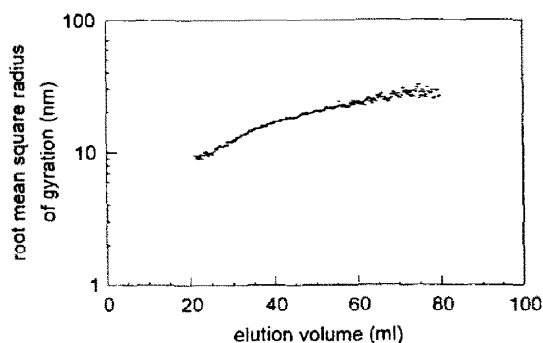not be measured because of the limitation in

Fig. 2. Radii of gyration of the polystyrene latex sample B1
as a function of the elution volume. The channel flow was 1.0
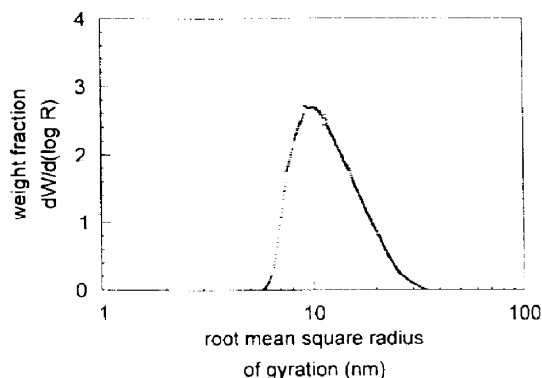ml min^{-1} and the cross-flow 2.0 ml min^{-1}.

Fig. 3. Differential distribution of the radius of gyration for the polystyrene latex sample B1.
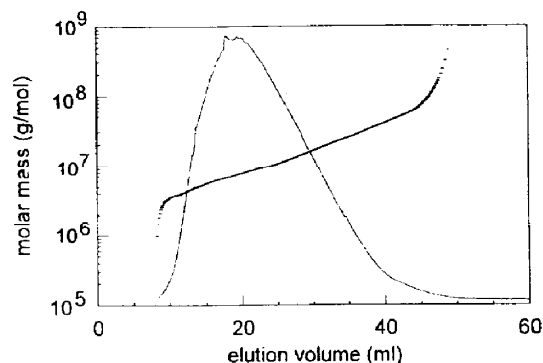

Fig. 4. Refractive index chromatogram and plot of molar masses of the polystyrene latex sample B1 determined by means of light-scattering measurements as a function of the elution volume.

light scattering was calculated by using a linear extrapolation in the radius versus mass plot. The data were used to determine the characteristic average values $\langle R_G^2 \rangle_n^{1/2}$, $\langle R_G^2 \rangle_w^{1/2}$ and $\langle R_G^2 \rangle_z^{1/2}$ by means of their definition relationships [22].The error values are the percentage standard deviations resulting from four measurements. The distribution function was used to determine the minimum, maximum and most frequent diameter, d_{LS}.

These values are compiled in Table 1 under the heading FFFF–MALLS. To verify these values, they are compared with Stokes diameters, d_S, from an FFFF–UV experiment on this sample. The FFFF–UV experiment was carried out by FFFractionation [32], who used FFFF to

separate the sample and a UV detector to monitor the eluate. In addition, Table 1 also includes the measured diffusion coefficients, D. Good agreement between the independently determined dimensions can be seen.

In Fig. 4 the refractive index chromatogram and the molar masses of the polystyrene latex sample determined by means of light scattering are represented as a function of the elution volume. With small elution volumes and correspondingly small particles the molar masses deviate to lower values. This behaviour must be a direct measure of the secondary instrument broadening that occurs in the system. Such instrumental broadening would be expected to

Table 1
Compilation of the dimensions of the polystyrene latex standard B1

Variable	FFFF–MALLS	FFFF–UV (254 nm)
$\langle R_G^2 \rangle_n^{1/2}$ (nm)	$10 \pm 10\%$	–
$\langle R_G^2 \rangle_w^{1/2}$ (nm)	$12 \pm 8\%$	–
$\langle R_G^2 \rangle_z^{1/2}$ (nm)	$15 \pm 7\%$	–
Maximum D (cm^2 s^{-1})	$2.9 \cdot 10^{-7}$	$2.9 \cdot 10^{-7}$
Most frequent D (cm^2 s^{-1})	$2.0 \cdot 10^{-7}$	$1.5 \cdot 10^{-7}$
Minimum D (cm^2 s^{-1})	$0.6 \cdot 10^{-7}$	$0.5 \cdot 10^{-7}$
Minimum diameter (nm)	$d_{LS} = 16$	$d_S = 16$
Most frequent diameter (nm)	$d_{LS} = 26$	$d_S = 28$
Maximum diameter (nm)	$d_{LS} = 85$	$d_S = 83$

The radii of gyration of the FFFF–MALLS experiments result from evaluation of the scattered light intensities, and the diameters d_{LS} were calculated from the radii of gyration. The FFFF–UV experiment was carried out by FFFractionation and yielded the Stokes diameters, d_S. The errors indicated correspond to the percentage standard deviation of the results from four experiments.
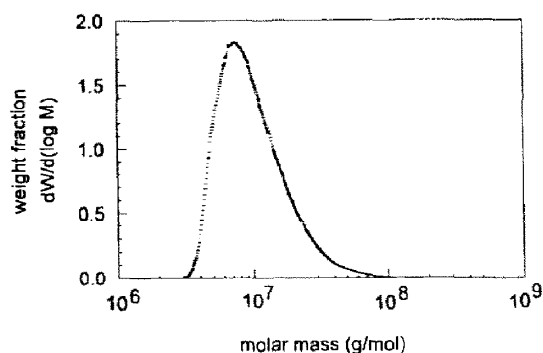
Fig. 5. Differential distribution of the molar mass for the polystyrene latex sample B1.

lower the molar mass by causing excessively high concentration values [31,33]. In the range of higher elution volumes and correspondingly large particles the molar masses deviate to higher values. This behaviour seems to be the result of the different sensitivities of the two detectors. In this range of low concentrations and large particles the light-scattering photometer, sensitive to molar mass, yields high signals whereas the differential refractometer yields no significant signal because of the very low concentration of the scattering particles.

The molar mass distribution represented in Fig. 5 was calculated by including the concen-

tration of each respective species. From this distribution it was possible to determine the number-average, weight-average and z-average molar masses, and also other characteristic values. These results and molar mass values from an FFFF–UV experiment are compiled in Table 2.

The measurements of the polystyrene latex standard show that the multi-angle laser light-scattering photometer is suitable for monitoring the eluate from the flow field-flow fractionator. The angular-dependent scattered light readings yield the absolutely determined radius of gyration and molar mass and, by including the respective concentrations, they also yield the distributions for these two variables. For lattices FFF provides absolute values for diffusion coefficients and hence, by employing the Stokes–Einstein relationship, also the absolute values for Stokes diameter and molar mass. In this way it is possible to determine the structural parameters of lattices independently of one another in a single experiment. Correlation of the results obtained by these two methods may be regarded as sufficiently accurate. However, it must be remembered that the procedure applied in the evaluation of the scattered light measurements contains two assumptions that are not fulfilled in the case of measurements on particles. The first assumption is that the wave front is not altered

Table 2
Compilation of the molar mass values for the polystyrene latex standard B1

Variable	FFFF–MALLS	FFFF–UV (254 nm)
M_n (g mol^{-1})	$7.3 \cdot 10^6 \pm 12\%$	–
M_w (g mol^{-1})	$13.4 \cdot 10^6 \pm 13\%$	–
M_z (g mol^{-1})	$32.1 \cdot 10^6 \pm 15\%$	–
M_w/M_n	1.8	–
M_z/M_n	4.4	–
Minimum M (g mol^{-1})	$2.9 \cdot 10^6$	$1.3 \cdot 10^6$
Most frequent M (g mol^{-1})	$7.1 \cdot 10^6$	$7.3 \cdot 10^6$
Maximum M (g mol^{-1})	$180 \cdot 10^6$	$190 \cdot 10^6$

The data from the FFFF–MALLS measurements result from scattered light measurements. The molar masses of the FFFF–UV experiment carried out by FFFractionation were calculated from the Stokes diameters.

on its passage through the sample and the second is that the difference in refractive index between sample and solvent is small.

4.2. Fractionation of a coil-shaped dissolved polymer

Dextrans are neutral, branched exopolysaccharides that are made enzymatically from sucrose. They are used as the base for manufacturing plasma expanders. In a three-dimensionally cross-linked form they serve as a separating medium in size-exclusion chromatography under the name Sephadex gel. This polymer was used for conducting trials on FFFF–MALLS as a means of characterizing coil-shaped dissolved polymers. In order to verify the results, the polymer was also characterized by means of SEC–MALLS.

The differential distribution of radius of gyration is represented in Fig. 6 and the differential distribution of molar mass in Fig. 7. The distributions were determined by means of FFFF/MALLS. It can be seen that this sample consists of a low-molar-mass fraction with a radius of gyration of ca. 20 nm and a molar mass of ca. $3.5 \cdot 10^5$ g mol^{-1}, and a high molar mass fraction with a radius of gyration of ca. 45 nm and a molar mass of ca. $3 \cdot 10^6$ g mol^{-1}.

Fig. 7. Comparative representation of the differential distribution of molar mass from SEC–MALLS and FFF–MALLS experiments on the polysaccharide standard dextran.

Fig. 6 shows also the radius of gyration distribution and Fig. 7 the molar mass distribution of the dextran sample obtained by means of SEC–MALLS. The steep high-molar-mass flank can clearly be seen on the right-hand side in this distribution function. It is caused by the exclusion boundary of the chromatographic system. Comparison of the results for the two methods of fractionation shows that the low-molar-mass flank of the distribution function determined by SEC with the selected column combination has a better resolution. On the other hand, the resolution of FFFF in the middle and high molar mass range is better. This is to be expected because the mass selectivity and upper working limit of FFFF are much higher [34]. However, the fractionation of high-molar-mass substances is the most important aspect of this experiment. Proof of good separation by FFFF is given by the correct slope in the graph of $\langle R_G^2 \rangle^{1/2}$ versus M in Fig. 9. There is no loss of substance or degradation during the measurements, as the weight-average molar masses, M_w, for both experiments determined by light scattering are the same, within the limit of error.

Table 3 gives a compilation of the data from SEC–MALLS and FFFF–MALLS experiments for comparative purposes. The respective mean values calculated for the radii and molar masses show a significantly weaker degree of separation
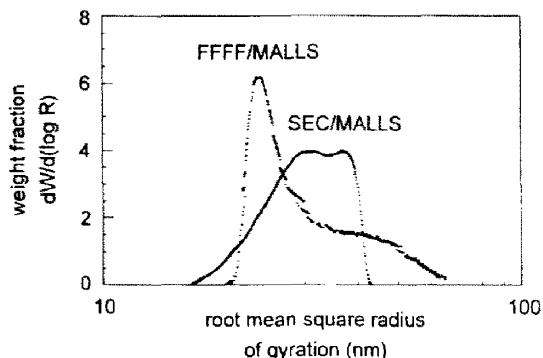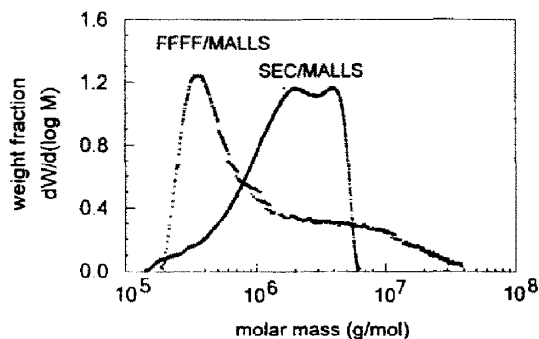

Fig. 6. Differential distribution of the radius of gyration for dextran, fractionation and detection were performed with FFFF–MALLS and SEC–MALLS. The channel flow was 1.0 ml min^{-1} and the cross-flow 0.7 ml min^{-1}.

Table 3
Compilation of the mean values of molar mass and radius of gyration for the dextran standard determined by FFFF–MALLS and SEC–MALLS

Variable	FFFF/MALLS	SEC/MALLS
M_n (g mol^{-1})	625 000 ± 14%	1 500 000 ± 8%
M_w (g mol^{-1})	2 730 000 ± 6%	2 680 000 ± 4%
M_z (g mol^{-1})	6 620 000 ± 9%	4 650 000 ± 6%
$\langle R_G^2 \rangle_n^{1/2}$ (nm)	29 ± 14%	40 ± 6%
$\langle R_G^2 \rangle_w^{1/2}$ (nm)	36 ± 6%	42 ± 5%
$\langle R_G^2 \rangle_z^{1/2}$ (nm)	47 ± 2%	44 ± 4%
M_w/M_n	4.4	1.8
M_z/M_n	10.6	3.1

The errors indicated correspond to the percentage standard deviation of the results from 10 experiments.

when compared with the results of FFFF–MALLS experiments. This results in the polydispersity being smaller by a factor of ca. 2.5. Within the limits of error for the two fractionation methods, the values of the weight-average molar mass, M_w, and the z-average radius of gyration, $\langle R_G^2 \rangle_z^{1/2}$, are the same. This is to be expected since light scattering yields precisely these moments of molar mass and radius of gyration for non-fractionated, and hence polydisperse, samples.

The investigations confirmed that this experimental set-up is able to determine distribution functions of the molar mass and the radius of gyration for dissolved polymers. The advantages of this set-up seems to lie in the applicability of FFFF, which is able to fractionate even problematic molecules of masses up to several 10^9 g mol^{-1} [34] combined with the high performance of the on-line MALLS photometer, which enables molar masses and radii of gyration to be measured absolutely.

4.3. Determination of the solution state

Performing an FFFF–MALLS experiment yields important data for polymer analysis in the form of distribution functions and means for the molar masses and radii of gyration. During the separation process, quasi-monodisperse fractions
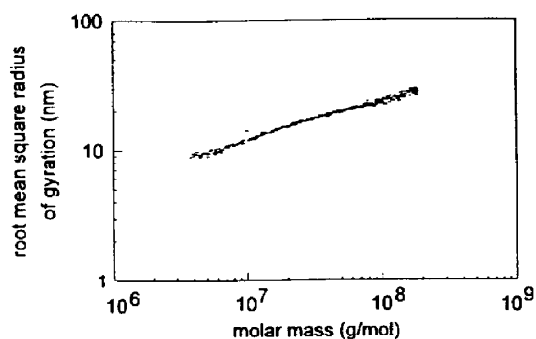

Fig. 8. Representation of the radii of gyration as a function of the molar mass for the polystyrene sample B1 in 0.05% (w/w) sodium dodecyl sulphate solution at 295 K, $\nu = 0.33$.

are characterized in terms of their molar mass and radius of gyration. These data can be used to establish a relationship between these two variables. The general form of such a relationship is given by

$$\langle R_G^2 \rangle^{1/2} = K_R M^{\nu} \qquad (10)$$

Like the radius of gyration, the Staudinger index is a measure of the volume of a dissolved polymer molecule with respect to its mass. This quantitative relationship given by the Kuhn–Mark–Houwink–Sakurada relationship, represented by the equation

$$[\eta] = K_\eta M^a \qquad (11)$$

Transformation from the form of Eq. 10 to that of Eq. 11 by means of the Flory–Fox theory [35] enables a comparison to be carried out of the experimental readings for the dextran with published Kuhn–Mark–Houwink–Sakurada relationships.

Table 4
Experimentally and theoretically derived $\langle R_G^2 \rangle^{1/2}$ versus M relationships for the polystyrene latex sample in 0.05% (w/w) sodium dodecyl sulphate solution

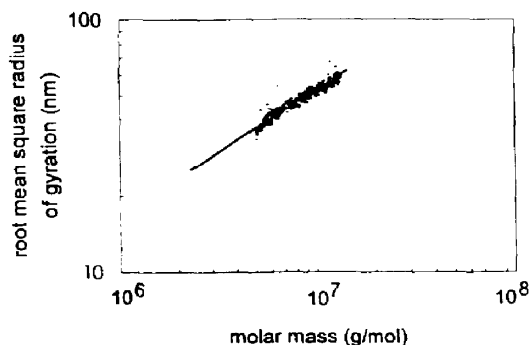| Source	Structure–property relationship
Experimental	$\langle R_G^2 \rangle^{1/2} = 0.055 M^{0.33}$ (nm)
Theoretical	$\langle R_G^2 \rangle^{1/2} = 0.056 M^{0.33}$ (nm)

Fig. 9. Graph of the radius of gyration of the polysaccharide dextran as a function of the molar mass in 0.1 M sodium nitrate solution at a temperature of 295 K, determined by SEC–MALLS and FFFF–MALLS.

In Fig. 8 the radii of gyration for the polystyrene latex sample are plotted against the molar masses in accordance with Eq. 10. The exponent ν was determined from the double-logarithmic plot. The pre-exponential factor K_R was determined by calculating the density of particles from the values of the measured radii and molar masses of the slices along the distribution. Table 4 provides a compilation of the experimental and a theoretical $\langle R_G^2 \rangle^{1/2}$ versus M relationship for rigid spheres. Good agreement can be seen.

Fig. 9 is a double-logarithmic plot of the $\langle R_G^2 \rangle^{0.5}$ versus M relationship for dextran. The solvent used was 0.1 M sodium nitrate solution containing 200 ppm of sodium azide. Measurements were carried out at a temperature of 295

K. The constant $K_R = 0.03$ and the exponent $\nu = 0.50 \pm 0.01$ were determined by linear extrapolation. Application of Flory–Fox-theory enabled the Kuhn–Mark–Houwink–Sakurada relationship to be calculated. For comparison this result is listed along with the corresponding literature data in Table 5 [36–41]. Good agreement can be seen between the experimentally determined values and the published data. These studies confirm that FFFF coupled with MALLS can also yield information about the solution state of the polymer.

Symbols

A_2	second virial coefficient
a	exponent of the $[\eta]$ versus M relationship
c	concentration
D	diffusion coefficient
d_{LS}	diameter calculated from the radius of gyration
dn/dc	refractive index increment
d_S	Stokes diameter
I	intensity of light
k	constant for light scattering with vertically polarized incident light
K_R	pre-exponential factor of the $\langle R_G^2 \rangle^{1/2}$ versus M relationship
K_η	pre-exponential factor of the $[\eta]$ versus M relationship
k	Boltzmann constant
M	molar mass
N_A	Avogadro's number
n	refractive index
$P_{(\vartheta)}$	scattering function
q	scattering vector
r	radius
R_ϑ	reduced scattered light intensity, Rayleigh ratio
$\langle R_G^2 \rangle^{1/2}$	root mean square radius of gyration
T	absolute temperature
t_R	retention time
V	scattering volume
$\dot{V}$	channel flow
$\dot{V}_x$	cross-flow

Table 5
Measured $\langle R_G^2 \rangle^{1/2}$ versus M and calculated $[\eta]$ versus M relationship and published data for dextrans

Source	Solvent	Structure–property relationship
This work	0.1 M NaNO$_3$	$\langle R_G^2 \rangle^{1/2} = 0.03 M^{0.50}$
		$[\eta] = 0.10 M^{0.50}$ [a]
[36]	0.1 M NaNO$_3$	$\langle R_G^2 \rangle^{1/2} \approx M^{0.48}$
[37]	0.1 M NaNO$_3$	$[\eta] = 0.37 M^{0.40}$
[38]	H$_2$O	$[\eta] = 0.12 M^{0.499}$
[39]	H$_2$O	$[\eta] = 0.17 M^{0.452}$
[40]	H$_2$O	$[\eta] = 0.10 M^{0.50}$
[41]	H$_2$O	$[\eta] = 0.05 M^{0.60}$

[a] Application of Flory–Fox theory.

Greek letters

η	viscosity
$[\eta]$	Staudinger index
ϑ	scattering angle
λ	wavelength of light
ν	Exponent of the $\langle R_G^2 \rangle^{1/2}$ versus M relationship

References

[1] W.-M. Kulicke (Editor), *Analysis of Polymers (Macromolecular Symposium Series)*, Hüthig and Wepf, Heidelberg, 1992.

[2] W.-M. Kulicke, J. Klein and R. Kniewske, *Prog. Polym. Sci.*, 8 (1982) 373.

[3] T. Griebel and W.-M. Kulicke, *Makromol. Chem.*, 193 (1992) 811.

[4] T. Griebel, W.-M. Kulicke and A. Hashemzadeh, *Colloid Polym. Sci.*, 269 (1991) 113.

[5] W.-M. Kulicke and H.-H. Hörl, *Colloid Polym. Sci.*, 263 (1985) 530.

[6] H.A. Adams and G. Hempelmann, *Anästhesiol. Intensivmed.*, 10 (1991) 277.

[7] W.-M. Kulicke, D. Roessner and W. Kull, *Starch/Stärke*, 45 (1993) 445.

[8] W.-M. Kulicke and N. Böse, *Colloid Polym. Sci.*, 262 (1984) 197.

[9] W.-M. Kulicke, S. Lenk, H.-D. Detzner and T. Weiss, *Chem.-Ing.-Tech.*, 5 (1993) 541.

[10] T. Griebel, W.-M. Kulicke and R. Kniewske, *J. Getreide Mehl Brot*, 5 (1992) 154.

[11] J.C. Giddings and M.H. Moon, *Anal. Chem.*, 64 (1992) 3029.

[12] W.W. Yau and J.J. Kirkland, *J. Chromatogr.*, 218 (1981) 217.

[13] J.C. Giddings, F.J.F. Yang and M.N. Myers, *Anal. Chem.*, 46 (1974) 1917.

[14] G. Liu and J.C. Giddings, *Chromatographia*, 34 (1992) 483.

[15] J.J. Kirkland and S.W. Rementer, *Anal. Chem.*, 64 (1992) 904.

[16] J.C. Giddings, L.K. Smith and M.N. Myers, *Anal. Chem.*, 48 (1976) 1587.

[17] J.J. Kirkland, C.H. Dilks and S.W. Rementer, *Anal. Chem.*, 64 (1992) 1295.

[18] M.A. Benincasa and J.C. Giddings, *Anal. Chem.*, 64 (1992) 790.

[19] J.J. Kirkland and C.H. Dilks, *Anal. Chem.*, 64 (1992) 2836.

[20] J.C. Giddings, M.A. Benincasa, M.K. Liu and P. Li, *Polym. Mater. Sci. Eng.*, 65 (1991) 21.

[21] S.K. Ratanathanawongs and J.C. Giddings, *Polym. Mater. Sci. Eng.*, 62 (1990) 181.

[22] P.J. Wyatt, *Anal. Chim. Acta*, 272 (1993) 1.

[23] A. Einstein, *Ann. Phys.*, 33 (1910) 1275.

[24] C.V. Raman, *Indian J. Phys.*, 2 (1927) 1.

[25] P. Debye, *J. Appl. Phys.*, 15 (1944) 338.

[26] B.H. Zimm, *J. Chem. Phys.*, 13 (1945) 141.

[27] J.J. Kirkland, C.H. Dilks, S.W. Rementer and W.W. Yau, *J. Chromatogr.*, 593 (1992) 339.

[28] M.-K. Liu, P.S. Williams, M.N. Myers and J.C. Giddings, *Anal. Chem.*, 63 (1991) 2115.

[29] K.G. Wahlund, H.S. Winegarner, K.D. Caldwall and J.C. Giddings, *Anal. Chem.*, 58 (1986) 573.

[30] M.T. Nguyen and R. Beckett, *Polym. Int.*, 30 (1993) 337.

[31] P.J. Wyatt and L.A. Papazian, *LC·GC*, 11 (1993) 862.

[32] *Instrument Manual for Model F-1000 Universal Fractionator*, FFFractionation, Salt Lake City, UT.

[33] P.J. Wyatt, *J. Chromatogr.*, 648 (1993) 27.

[34] K.D. Caldwell, *Anal. Chem.*, 60 (1988) 959A.

[35] P.J. Flory and T.G. Fox, *J. Am. Chem. Soc.*, 73 (1951) 1904.

[36] J.A.M. Smit, J.A.P.P. van Dijk, M.G. Mennen and M. Daoud, *Macromolecules*, 25 (1992) 3585.

[37] B. Tinland, J. Mazet and M. Rinaudo, *Makromol. Chem. Rapid Commun.*, 9 (1988) 69.

[38] A.M. Basedow, K.H. Ebert, H. Ederer and H. Hunger, *Makromol. Chem.*, 177 (1976) 1501.

[39] *Pharmacosmos Dextran Standards*, Pharmacosmos, Viby, 1988.

[40] F.R. Senti, N.N. Hellman, N.H. Ludwig, G.E. Babcock, R. Tobin and C.A. Class, *J. Polym. Sci.*, 17 (1955) 527.

[41] K. Gekko and H. Noguchi, *Biopolymers*, 10 (1971) 1513.